J Nanostruct 16(3): 3126-3135, Summer 2026

RESEARCH PAPER

Analytical and Environmental Assessment of a Novel GO/Poly(Acrylic Acid-co-Maleic Anhydride) Nanocomposite Hydrogel for the Adsorptive Removal of Fuchsin Basic Dye from Wastewater

*Ziyad T. Al-Khateeb [1] *, Ameer Jaber [2], Abtisam Jasim Abbas [2]*

[1] *Department of Chemistry, College of Science, University of Al-Qadisiyah, Diwaniya, Iraq*

[2] *Department of Environment, College of Science – University of Al-Qadisiyah, Iraq*

ARTICLE INFO

Article History:
Received 08 March 2026
Accepted 11 May 2026
Published 01 July 2026

Keywords:
Adsorption
Graphene oxide
Kinetics
Thermodynamics
Water treatment

ABSTRACT

Water pollution caused by synthetic dyes continues to attract serious attention from environmental researchers, particularly because many of these compounds are toxic, non-biodegradable, and remain in aquatic systems for long periods of time. This study developed a nanocomposite hydrogel utilising graphene oxide and a copolymer of acrylic acid and maleic anhydride, designated as GO/P(AA-MA), through free radical polymerisation. Its efficacy as an adsorbent for Fuchsin Basic (FB), a cationic dye commonly used in the textile industry and biological staining, was assessed. Fourier-transform infrared spectroscopy (FTIR), X-ray diffraction (XRD), and field-emission scanning electron microscopy (FESEM) were used to study the synthesised material. These tests showed that GO was successfully added to the polymer matrix and that the material had a rough, porous shape that was good for dye uptake. Batch experiments were conducted to investigate the influence of contact time, initial dye concentration, adsorbent mass, pH, ionic strength, and temperature on the adsorption behaviour. Kinetic data fitted the pseudo-second-order model very well ($R^2 > 0.99$), while equilibrium data were best described by the Langmuir isotherm, giving a maximum monolayer capacity of about 285 mg g^{-1} at 298 K. Thermodynamic analysis indicated that the process is spontaneous, endothermic, and entropy-driven. The adsorbent was further tested over five adsorption–desorption cycles with only a modest loss of efficiency, which suggests that GO/P(AA-MA) is a promising and reusable material for the treatment of dye-contaminated water.

How to cite this article
Al-Khateeb Z., Jaber A., Abbas A. Analytical and Environmental Assessment of a Novel GO/Poly(Acrylic Acid-co-Maleic Anhydride) Nanocomposite Hydrogel for the Adsorptive Removal of Fuchsin Basic Dye from Wastewater. J Nanostruct, 2026; 16(3):3126-3135. DOI: 10.22052/JNS.2026.03.009

INTRODUCTION

The rapid expansion of industrial activities, especially in the textile, leather, paper, cosmetic, and pharmaceutical sectors, has led to the release of huge amounts of coloured wastewater into natural water bodies [1,2]. Even at very low concentrations, synthetic dyes can impair light penetration, disturb aquatic ecosystems, and

* *Corresponding Author Email: ziyad.tariq@qu.edu.iq*

pose serious risks to human health due to their mutagenic and, in some cases, carcinogenic nature [3]. Fuchsin Basic (FB) — also known as basic fuchsin or rosaniline hydrochloride — is a triphenylmethane cationic dye which is commonly used for staining bacteria and for colouring textile fibres [4]. It is highly stable, water-soluble, and difficult to remove by conventional biological treatment processes [5].

Adsorption is still one of the best ways to remove dye, even if there are many others, such as coagulation-flocculation, membrane filtering, advanced oxidation, photocatalysis, and electrochemical therapy. This is mainly due to its simplicity of operation, low running cost, and relatively high efficiency [6,7]. There are many various kinds of adsorbents that have been written about in the literature. Some examples are activated carbon, clays, charcoal, zeolites, and different kinds of polymeric hydrogels [8–10]. Hydrogels, in particular, have a customisable three-dimensional polymeric network and a lot of functional groups that can strongly interact with dye molecules [11].

Graphene oxide (GO) has recently emerged as an excellent adsorbent precursor thanks to its very large specific surface area, its abundant oxygen-containing functional groups (–OH, –COOH, epoxy), and its ability to form π–π interactions with aromatic pollutants [12,13]. However, pure GO tends to aggregate in aqueous media and is usually difficult to recover after use. Embedding GO into a polymer network, for instance a copolymer of acrylic acid and maleic anhydride, can provide additional anionic sites for capturing cationic dyes such as FB, while also offering mechanical stability to the adsorbent [14,15]. In this context, the present work was designed to prepare a GO/P(AA-MA) nanocomposite hydrogel and to investigate its behaviour for the removal of FB from aqueous solutions, with particular attention given to the kinetics, isotherms, thermodynamics, and reusability.

MATERIALS AND METHODS

Materials

Acrylic acid (AA, ≥ 99%), maleic anhydride (MA, ≥ 98%), N,N′-methylenebisacrylamide (MBA, used as cross-linker), potassium persulfate (KPS, initiator), sodium hydroxide (NaOH), hydrochloric acid (HCl), sodium chloride (NaCl), and Fuchsin Basic dye (molecular formula $C_{20}H_{20}ClN_3$; molecular weight 337.86 g mol^{-1}) were purchased from Sigma-Aldrich and used without further purification. Graphene oxide was prepared in our laboratory from graphite powder by a modified Hummers method, as described in an earlier report [16]. All solutions were prepared using distilled water.

Preparation of the GO/P(AA-MA) nanocomposite

The nanocomposite hydrogel was synthesized by free radical polymerization in an aqueous medium. In a typical procedure, 10 mL of AA was partially neutralized (~60%) with NaOH solution under continuous stirring and then mixed with 1.5 g of MA in a three-necked flask. An aqueous dispersion of GO (0.05 g in 10 mL of distilled water) was sonicated for 20 min and added dropwise to the monomer mixture under vigorous stirring in order to promote good dispersion. After that, 0.1 g of MBA and 0.15 g of KPS (previously dissolved in 5 mL of water) were added, and the mixture was transferred to a water bath set at 70 °C for 4 h under a nitrogen atmosphere. The obtained gel was cut into small pieces, washed several times with distilled water and then with ethanol to remove any unreacted species, dried in an oven at 50 °C until constant weight, and finally ground and stored in a desiccator.

Characterization

The functional groups present in GO, P(AA-MA), and the GO/P(AA-MA) nanocomposite were identified using a Shimadzu IR Prestige-21 FTIR spectrometer in the wavenumber range 4000–400 cm^{-1} (KBr pellet method). The crystalline structure of the samples was analysed by X-ray diffraction using a Shimadzu XRD-6000 instrument with Cu Kα radiation (λ = 1.5406 Å) over the 2θ range 5–60° at a scanning rate of 2° min^{-1}. The surface morphology was examined using a TESCAN MIRA3 field-emission scanning electron microscope after sputter-coating the samples with a thin gold layer.

Batch adsorption experiments

A stock solution of FB (1000 mg L^{-1}) was prepared by dissolving an appropriate amount of the dye in distilled water, and the working solutions were obtained by successive dilution. In a typical experiment, 0.05 g of the nanocomposite was added to 50 mL of dye solution of known concentration in a 100 mL conical flask, and the mixture was shaken at 200 rpm in a thermostatic water-bath shaker. Samples were withdrawn at

pre-set time intervals, centrifuged for 5 min at 4000 rpm, and the residual dye concentration was determined spectrophotometrically at λmax = 545 nm.

The removal efficiency (R %) and the adsorption capacity (qt, mg g^{-1}) were calculated according to:

$$R\,\% = [(C_0 - C_t)/C_0] \times 100 \quad (1)$$

$$q_t = [(C_0 - C_t) \times V] / m \quad (2)$$

where C_o and C_t (mg L^{-1}) are the dye concentrations at the initial time and at time t, respectively, V is the volume of the solution (L), and m is the mass of the adsorbent (g).

Systematic investigations were conducted on the effects of contact time (5-180 min), starting dye concentration (25-300mg.L^{-1}), adsorbent dosage (0.01-0.1 g), pH (2-10), ionic strength (0-0.5M NaCl), and temperature (288-318K). HCl (0.1M) and NaOH (0.1M) solutions used to change the pH. For regeneration tests, the utilised nanocomposite was washed with 0.1M HCl and then with distilled water until the pH was neutral. It was then dried and used for five more cycles.

Swelling study

The swelling behaviour of the nanocomposite was measured gravimetrically. A known mass of dry hydrogel (m_d) was immersed in distilled water at room temperature. At given time intervals, the swollen sample was removed, gently blotted with filter paper to eliminate excess surface water, and weighed (m_s). The swelling ratio (SR) was calculated as:

$$SR = (m_s - m_d) / m_d \quad (3)$$

RESULTS AND DISCUSSION

Characterization of the nanocomposite

Fig. 1 shows the key characterisation data for the materials that were made. These include the FTIR spectra, XRD patterns, and FESEM micrographs of GO, pure P(AA-MA), and the

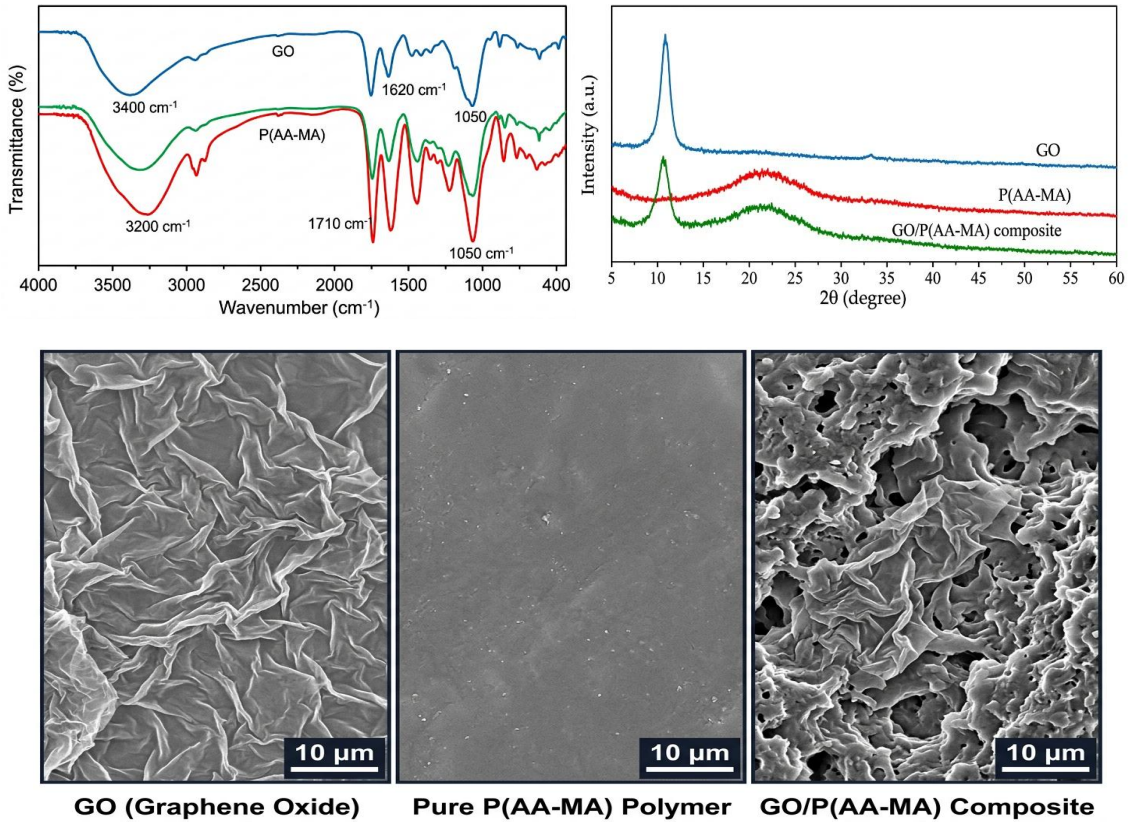

Fig. 1. FTIR spectra, XRD patterns, and FESEM images of GO, P(AA-MA), and GO/P(AA-MA) nanocomposite.

final GO/P(AA-MA) nanocomposite. The FTIR spectrum of GO shows a broad band around 3400 cm^{-1} that is caused by the stretching vibration of –OH groups. The peaks at 1720, 1620, and 1050 cm^{-1} are due to the C=O of carboxylic groups, the aromatic C=C skeletal vibration, and the C–O of epoxy/alkoxy groups, respectively [17]. The spectrum of P(AA-MA) displays typical absorption bands of carboxylic groups near 1710 cm^{-1} and a broad –OH band centred around 3200 cm^{-1}. In the composite, most of the characteristic peaks of both components are still visible, though with some slight shifts and broadening, which is consistent with the formation of hydrogen bonds and possible esterification reactions between the oxygen-containing groups of GO and the –COOH/–OH groups of the copolymer [18].

The XRD pattern of GO (Fig. 1b) shows the characteristic sharp peak at 2θ ≈ 10.5° corresponding to the (001) reflection, which gives an interlayer spacing close to 0.84 nm [19]. Pure P(AA-MA) exhibits a broad amorphous halo centred near 2θ ≈ 22°, which is typical of polymeric hydrogels. In the nanocomposite, the sharp peak of GO is strongly weakened and shifted to a slightly lower angle, suggesting that

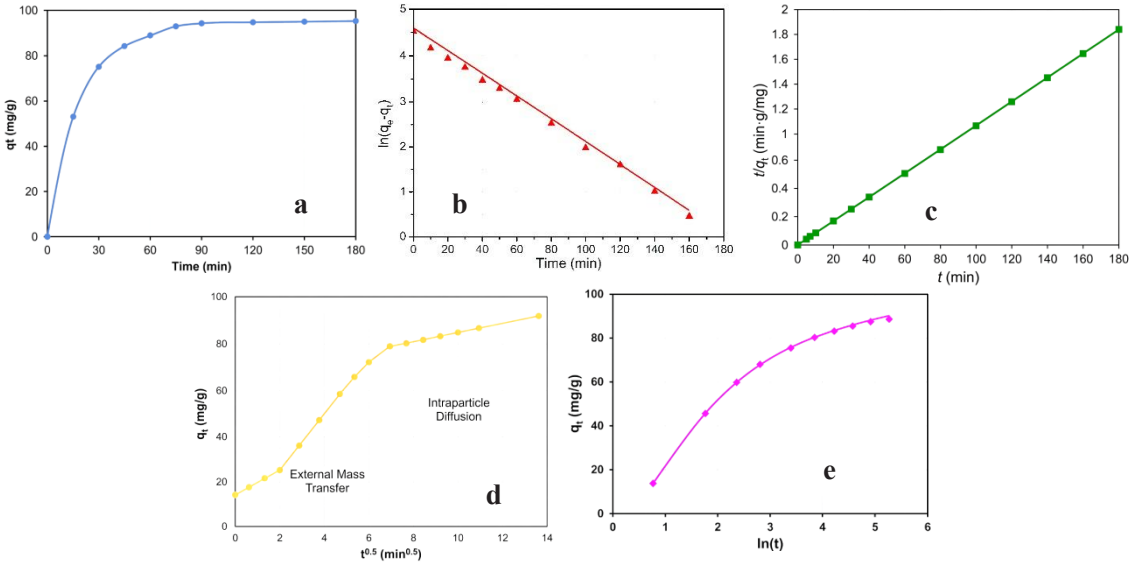

Fig. 2. Kinetic study of FB adsorption onto GO/P(AA-MA): (a) effect of contact time; (b) pseudo-first-order plot; (c) pseudo-second-order plot; (d) Elovich plot; (e) intraparticle (Weber–Morris) diffusion plot.

Table 1. Kinetic parameters for the adsorption of FB onto GO/P(AA-MA) at 298 K.

Kinetic model	Parameter	Value
Experimental	q_e, exp (mg g^{-1})	92.40
Pseudo-first-order	q_e, cal (mg g^{-1})	54.72
	k_1 (min^{-1})	0.0386
	R^2	0.9427
Pseudo-second-order	q_e, cal (mg g^{-1})	94.79
	k_2 (g mg^{-1} min^{-1})	1.52×10^{-3}
	R^2	0.9988
Elovich	α (mg g^{-1} min^{-1})	28.64
	β (g mg^{-1})	0.0763
	R^2	0.9614
Intraparticle diffusion	k_id (mg g^{-1} $min^{-0.5}$)	6.23
	C (mg g^{-1})	37.80
	R^2	0.9125

GO sheets are exfoliated and well dispersed inside the polymer network rather than forming aggregated stacks [20]. FESEM images (Fig. 1c) confirm these observations: pure GO shows the expected wrinkled sheet-like morphology, P(AA-MA) appears relatively smooth with few surface features, whereas the composite displays a rougher and more porous texture, in which GO sheets seem embedded within the polymer. Such a surface is expected to increase the number of accessible adsorption sites and to improve dye diffusion inside the matrix.

Effect of contact time and adsorption kinetics

The influence of contact time on the uptake of FB was evaluated at an initial dye concentration of 100mg.L^{-1}, keeping all other parameters constant. As illustrated in Fig. 2a, the adsorption was rapid during the first 30min., then slowed gradually, and finally reached equilibrium at around 90 min. This type of profile, which has been observed for many hydrogel-type adsorbents, is generally attributed to the abundance of free active sites in the early stage of the process, which become progressively saturated with time [21].

In order to describe the mechanism of adsorption, four well-known kinetic models were applied to the experimental data: the pseudo-first-order (PFO), pseudo-second-order (PSO), Elovich, and the intraparticle diffusion (Weber–Morris) models, expressed as follows:

$$\ln(q_e - q_t) = \ln q_e - k_1 t \quad (4)$$

$$t/q_t = 1/(k_2 q_e^2) + t/q_e \quad (5)$$

$$q_t = (1/\beta)\ln(\alpha\beta) + (1/\beta)\ln t \quad (6)$$

$$q_t = k_{id} t^{0.5} + C \quad (7)$$

The linear plots corresponding to these four models are shown in Fig. 2b-e, and the estimated kinetic parameters together with the correlation coefficients are summarized in Table 1. Among the tested models, the pseudo-second-order model gave the highest correlation coefficient ($R^2 > 0.99$) and the calculated qe values were in excellent agreement with the experimental ones. This outcome suggests that the adsorption of FB on GO/P(AA-MA) is governed by a chemisorption-type mechanism, which most likely involves electrostatic attraction and hydrogen bonding between the positively charged dye and the deprotonated -COO$^-$ groups of the nanocomposite [22]. The Weber-Morris plot (Fig. 2e) was not a single straight line passing through the origin; instead, at least two linear segments were observed, which indicates that more than one step controls the overall rate, namely external (film) diffusion during the first stage and intraparticle diffusion at longer times [23].

Effect of initial concentration and adsorption isotherms

The equilibrium uptake increased from about 48 to 265 mg g^{-1} when the initial dye concentration was raised from 25 to 300 mg L^{-1}, while the

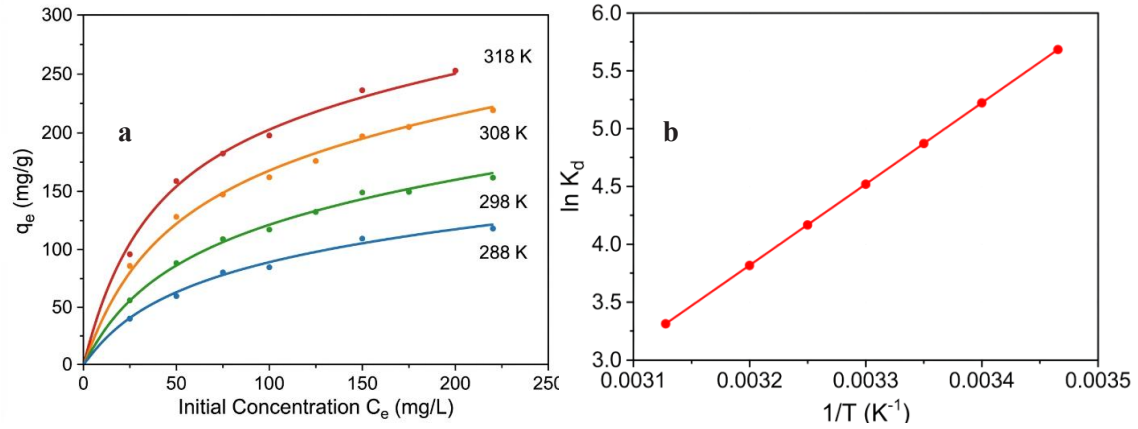

Fig. 3. (a) Effect of temperature on the adsorption of FB onto GO/P(AA-MA); (b) van't Hoff plot used for the determination of the thermodynamic parameters.

removal percentage showed the opposite trend. This behaviour, which is often reported in the literature, can be explained by the fact that a higher concentration provides a stronger driving force that helps to overcome the mass-transfer resistance between the solution and the solid surface, although the finite number of active sites cannot capture all the dye molecules at high loadings, which leads to a decrease of the percentage removal [24].

The equilibrium data were then analysed using four classical isotherm models — Langmuir, Freundlich, Temkin, and Dubinin–Radushkevich (D-R) — whose linearized forms are given below:

$$C_e/q_e = 1/(q_{max}\, K_L) + C_e/q_{max} \quad (8)$$

$$\ln q_e = \ln K_F + (1/n) \ln C_e \quad (9)$$

$$q_e = B \ln K_T + B \ln C_e \quad (10)$$

$$\ln q_e = \ln q_D - \beta\, \varepsilon^2 \quad (11)$$

Table 2 shows the computed isotherm parameters and correlation coefficients. The Langmuir model fit the experimental data best, with a R^2 value of almost 0.998. It also showed that the maximum adsorption capacity (qmax) was about 285 mg g^{-1} at 298 K. This means that FB typically sticks to places where the energy is the same, which makes a single layer of coverage on the surface of the nanocomposite [25]. The dimensionless separation factor R_L, calculated from $R_L = 1/(1 + K_L C_o)$, was between 0 and 1 in all cases, indicating favourable adsorption. The Freundlich exponent 1/n was smaller than unity, which is again consistent with a favourable process [26]. The mean adsorption energy E, estimated from the D-R model, was in the range 8–12 kJ mol^{-1}, suggesting that the interaction between FB and the nanocomposite is of an intermediate nature, somewhere between pure physical adsorption and ion-exchange/chemisorption.

Effect of temperature and thermodynamic study

The role of temperature in the adsorption process was investigated between 288 and 318 K, while keeping the other parameters constant. As shown in Fig. 3a, the amount of dye adsorbed at equilibrium increased with increasing

Table 2. Isotherm parameters for the adsorption of FB onto GO/P(AA-MA) at 298 K.

Isotherm model	Parameter	Value
Langmuir	q_{max} (mg g^{-1})	285.7
	K_L (L mg^{-1})	0.0721
	R_L	0.044 – 0.357
	R^2	0.9982
Freundlich	K_F (mg g^{-1})(L mg^{-1})^(1/n)	42.58
	n	2.86
	1/n	0.3497
	R^2	0.9214
Temkin	K_t (L g^{-1})	1.824
	B (J mol^{-1})	47.35
	b_t (J mol^{-1})	52.34
	R^2	0.9547
Dubinin–Radushkevich	q_D (mg g^{-1})	247.3
	β (mol^2 kJ^{-2})	6.78×10^{-9}
	E (kJ mol^{-1})	8.59
	R^2	0.8962

Table 3. Thermodynamic parameters for the adsorption of FB onto GO/P(AA-MA).

T (K)	K_D (L g^{-1})	ΔG° (kJ mol^{-1})	ΔH° (kJ mol^{-1})	ΔS° (J mol^{-1} K^{-1})
288	3.57	−3.05		
298	5.04	−4.01	+24.60	+96.00
308	6.96	−4.97		
318	9.42	−5.93		

temperature, which is typical of an endothermic process and may be related to an enhanced mobility of the dye molecules and/or an opening of the polymer network at higher temperatures [27].

Thermodynamic parameters — the Gibbs free energy (ΔG°), enthalpy (ΔH°), and entropy (ΔS°) — were estimated using the following equations:

$$\Delta G^\circ = -RT \ln K_d \quad (12)$$

$$\ln K_d = (\Delta S^\circ/R) - (\Delta H^\circ/RT) \quad (13)$$

where $K_d = q_e/C_e$ is the distribution coefficient, R is the universal gas constant (8.314 J mol^{-1} K^{-1}), and T is the absolute temperature (K). The computed values are presented in Table 3, and the corresponding van't Hoff plot (ln K_d vs 1/T) is displayed in Fig. 3b.

The ΔG° values were negative at all temperatures and became more negative as the temperature increased, which confirms that the adsorption of FB on GO/P(AA-MA) is a spontaneous and thermodynamically favourable process. A positive ΔH° value (+24.6 kJ mol^{-1}) indicates that the process is endothermic in nature. The positive value of ΔS° (+96 J mol^{-1} K^{-1}) reflects an increase in the randomness at the solid–liquid interface, which is usually associated with the release of hydration water molecules surrounding the charged sites of the adsorbent once the dye molecules are fixed onto them [28].

Effect of pH, ionic strength, and swelling behaviour

The solution pH is a crucial variable in dye adsorption, because it controls both the surface charge of the adsorbent and the ionization state of the dye molecules [29]. As illustrated in Fig. 4a, the removal of FB was low in strongly acidic media (pH 2) and increased considerably when the pH was raised up to 7–8, after which a slight decrease was noticed. At low pH values, the carboxylic groups of

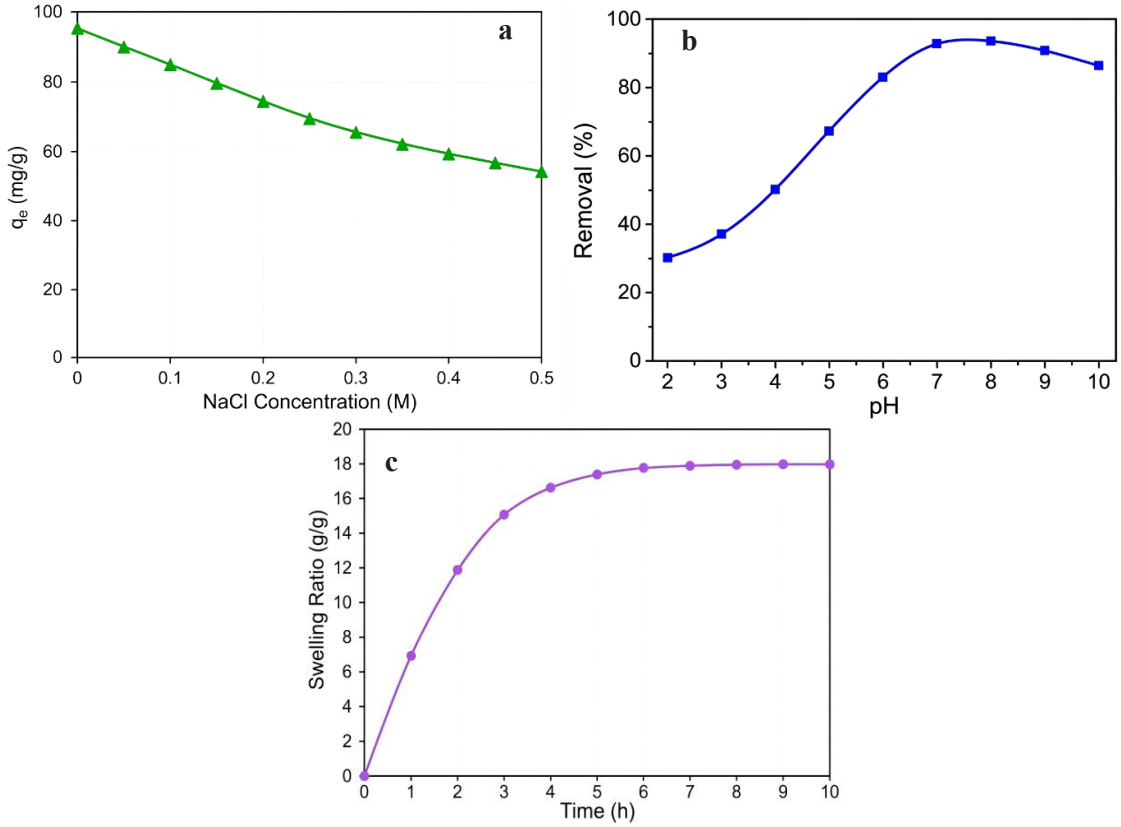

Fig. 4. Effect of operating variables on FB adsorption by GO/P(AA-MA): (a) solution pH; (b) ionic strength (NaCl concentration); (c) swelling behaviour in distilled water.

the nanocomposite are mostly in their protonated form (–COOH), so the electrostatic attraction toward the cationic FB is suppressed; in addition, the excess of H^+ competes with the dye cations for the available sites. With increasing pH, –COOH groups are progressively converted into $–COO^–$, which strongly attract the positively charged FB molecules through electrostatic interaction [30]. The small drop observed above pH 9–10 may be attributed to competition with $OH^–$ ions and to a possible change in the ionization state of the dye itself.

The effect of ionic strength was examined by varying the NaCl concentration from 0 to 0.5 M (Fig. 4b). A clear decrease of the adsorption capacity was noticed when the salt concentration was increased. Two main reasons can be advanced to explain this behaviour. First, Na^+ ions compete with FB cations for the negatively charged sites of the nanocomposite; second, the high ionic strength partly screens the electrostatic interaction between the dye and the adsorbent. The fact that this effect is relatively pronounced supports the idea that electrostatic interactions play an important role in the adsorption mechanism, although they are not the only contribution since a significant uptake is still observed even at high salt concentrations [31].

The swelling behaviour of the nanocomposite is shown in Fig. 4c. The swelling ratio increased

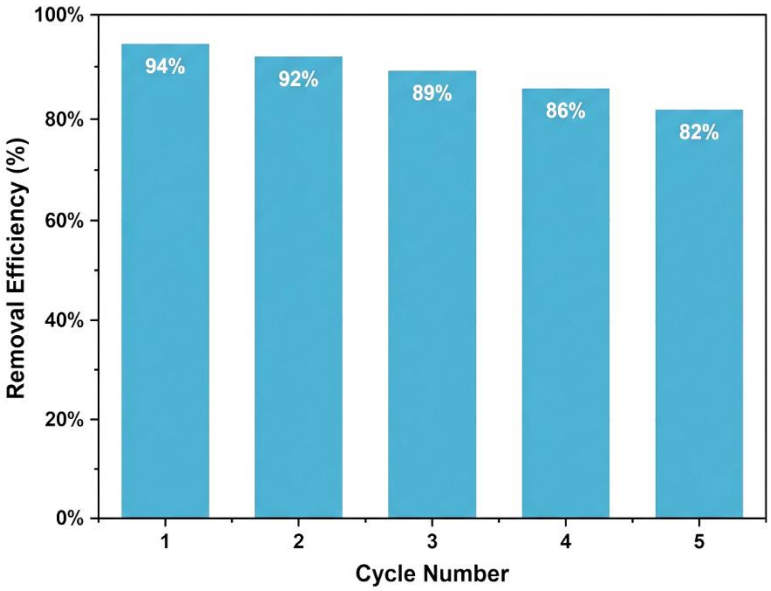

Fig. 5. Regeneration and reusability of GO/P(AA-MA) nanocomposite for FB removal over five consecutive cycles.

Table 4. Comparison of the maximum adsorption capacity of GO/P(AA-MA) with other adsorbents reported in the literature for FB and related cationic dyes.

Adsorbent	Dye	q_{max} (mg g^{-1})	Reference
Activated carbon	Fuchsin Basic	137.2	[10]
Bentonite	Fuchsin Basic	68.7	[8]
Zeolite	Fuchsin Basic	45.9	[9]
Fly ash	Basic Fuchsin	39.8	[24]
Graphene oxide nanosheets	Fuchsin Basic	204.5	[28]
Cellulose-based hydrogel	Basic Fuchsin	152.6	[15]
Chitosan-based composite	Fuchsin Basic	176.4	[11]
Pine cone powder	Basic cationic dye	98.3	[30]
GO/P(AA-MA) nanocomposite	Fuchsin Basic	285.7	This study

sharply during the first 3 h, then rose more slowly, and reached a plateau after about 6 h with an equilibrium value of ~18 g g^{-1}. Such a pronounced swelling is directly related to the presence of hydrophilic –COOH/–COO^- groups in the polymer network and to the oxygen-containing functionalities on GO sheets, which together favour the diffusion of water into the matrix [32]. A high swelling degree is a valuable feature for adsorption, since it facilitates the diffusion of dye molecules through the hydrogel and enhances the contact with the internal active sites.

Regeneration and reusability

From a practical and economic point of view, the ability to regenerate and reuse an adsorbent is a key feature that determines its suitability for real applications [33]. In this work, the spent nanocomposite was regenerated by washing with 0.1 M HCl, followed by rinsing with distilled water until neutral pH, and finally drying before being used again. The results obtained over five consecutive adsorption–desorption cycles are presented in Fig. 5. The removal efficiency decreased only slightly from about 94 % in the first cycle to about 82 % in the fifth cycle, which corresponds to a total drop of less than 13 %.

The small decrease observed after several cycles can be ascribed to the incomplete desorption of strongly adsorbed dye molecules from the internal sites of the network, and possibly to a minor loss of active sites and/or of mass during the handling steps. Overall, these results clearly indicate that GO/P(AA-MA) maintains a good adsorption capacity after several cycles and can therefore be regarded as a reusable and economically reasonable adsorbent for the removal of FB dye from contaminated water.

Comparison with other adsorbents

To place the present results in a broader perspective, the maximum adsorption capacity obtained for FB on GO/P(AA-MA) was compared with the values reported in the literature for other adsorbents towards Fuchsin Basic and similar cationic dyes (Table 4). The capacity obtained in this study (~285 mg g^{-1}) is comparable to, or higher than, that of many previously reported materials, which confirms that the combination of GO with the P(AA-MA) network provides an effective platform for the uptake of cationic dyes.

CONCLUSION

This paper made a new nanocomposite hydrogel called GO/P(AA-MA) via free radical polymerisation. They then used it to remove Fuchsin Basic dye from water. FTIR, XRD, and FESEM tests showed that GO was well integrated into the polymer network and that the final material had a rough and porous surface with a lot of functional groups. Batch adsorption investigations demonstrated that the absorption of FB is significantly affected by contact time, starting concentration, pH, ionic strength, and temperature. The kinetic study showed that the process followed the pseudo-second-order model. The Langmuir isotherm best characterised the equilibrium data, with a maximum adsorption capacity of roughly 285 mg g^{-1} at 298 K. Thermodynamic calculations showed that the process happens on its own, takes in energy, and is driven by entropy. The composite also had a high swelling ratio and worked well during five regeneration cycles, with only a small drop in efficiency. Taken together, these findings indicate that GO/P(AA-MA) is a promising, low-cost, and reusable adsorbent that could be developed further for the treatment of real dye-containing wastewater.

CONFLICT OF INTEREST

The authors declare that there is no conflict of interests regarding the publication of this manuscript.

REFERENCES

1. Forgacs E, Cserháti T, Oros G. Removal of synthetic dyes from wastewaters: a review. Environ Int. 2004;30(7):953-971.
2. Crini G. Non-conventional low-cost adsorbents for dye removal: A review. Bioresour Technol. 2006;97(9):1061-1085.
3. Rafatullah M, Sulaiman O, Hashim R, Ahmad A. Adsorption of methylene blue on low-cost adsorbents: A review. J Hazard Mater. 2010;177(1-3):70-80.
4. Mittal A, Kaur D, Mittal J. Applicability of waste materials—bottom ash and deoiled soya—as adsorbents for the removal and recovery of a hazardous dye, brilliant green. Journal of Colloid and Interface Science. 2008;326(1):8-17.
5. Gupta VK, Suhas. Application of low-cost adsorbents for dye removal – A review. J Environ Manage. 2009;90(8):2313-2342.
6. Robinson T, McMullan G, Marchant R, Nigam P. Remediation of dyes in textile effluent: a critical review on current treatment technologies with a proposed alternative. Bioresour Technol. 2001;77(3):247-255.
7. Ali I. New Generation Adsorbents for Water Treatment. Chem Rev. 2012;112(10):5073-5091.
8. Bhatnagar A, Sillanpää M. Utilization of agro-industrial and

municipal waste materials as potential adsorbents for water treatment—A review. Chem Eng J. 2010;157(2-3):277-296.
9. Zhu M-X, Lee L, Wang H-H, Wang Z. Removal of an anionic dye by adsorption/precipitation processes using alkaline white mud. J Hazard Mater. 2007;149(3):735-741.
10. El Qada EN, Allen SJ, Walker GM. Adsorption of Methylene Blue onto activated carbon produced from steam activated bituminous coal: A study of equilibrium adsorption isotherm. Chem Eng J. 2006;124(1-3):103-110.
11. Ahmed EM. Hydrogel: Preparation, characterization, and applications: A review. Journal of Advanced Research. 2015;6(2):105-121.
12. Chowdhury S, Balasubramanian R. Recent advances in the use of graphene-family nanoadsorbents for removal of toxic pollutants from wastewater. Advances in Colloid and Interface Science. 2014;204:35-56.
13. Wang J, Chen B, Xing B. Wrinkles and Folds of Activated Graphene Nanosheets as Fast and Efficient Adsorptive Sites for Hydrophobic Organic Contaminants. Environmental Science and Technology. 2016;50(7):3798-3808.
14. Zhao G, Li J, Ren X, Chen C, Wang X. Few-Layered Graphene Oxide Nanosheets As Superior Sorbents for Heavy Metal Ion Pollution Management. Environmental Science and Technology. 2011;45(24):10454-10462.
15. Liu L, Gao ZY, Su XP, Chen X, Jiang L, Yao JM. Adsorption Removal of Dyes from Single and Binary Solutions Using a Cellulose-based Bioadsorbent. ACS Sustainable Chemistry and Engineering. 2015;3(3):432-442.
16. Marcano DC, Kosynkin DV, Berlin JM, Sinitskii A, Sun Z, Slesarev A, et al. Improved Synthesis of Graphene Oxide. ACS Nano. 2010;4(8):4806-4814.
17. Li Y, Du Q, Liu T, Peng X, Wang J, Sun J, et al. Comparative study of methylene blue dye adsorption onto activated carbon, graphene oxide, and carbon nanotubes. Chem Eng Res Des. 2013;91(2):361-368.
18. Yan H, Tao X, Yang Z, Li K, Yang H, Li A, et al. Effects of the oxidation degree of graphene oxide on the adsorption of methylene blue. J Hazard Mater. 2014;268:191-198.
19. Stankovich S, Dikin DA, Piner RD, Kohlhaas KA, Kleinhammes A, Jia Y, et al. Synthesis of graphene-based nanosheets via chemical reduction of exfoliated graphite oxide. Carbon. 2007;45(7):1558-1565.
20. Zhao Y, Chen H, Li J, Chen C. Hierarchical MWCNTs/Fe 3 O 4 /PANI magnetic composite as adsorbent for methyl orange removal. Journal of Colloid and Interface Science. 2015;450:189-195.
21. Ho YS, McKay G. Pseudo-second order model for sorption processes. Process Biochem. 1999;34(5):451-465.
22. Azizian S. Kinetic models of sorption: a theoretical analysis. Journal of Colloid and Interface Science. 2004;276(1):47-52.
23. Weber WJ, Morris JC. Kinetics of Adsorption on Carbon from Solution. Journal of the Sanitary Engineering Division. 1963;89(2):31-59.
24. Mall ID, Srivastava VC, Agarwal NK, Mishra IM. Adsorptive removal of malachite green dye from aqueous solution by bagasse fly ash and activated carbon-kinetic study and equilibrium isotherm analyses. Colloids Surf Physicochem Eng Aspects. 2005;264(1-3):17-28.
25. Langmuir I. THE ADSORPTION OF GASES ON PLANE SURFACES OF GLASS, MICA AND PLATINUM. Journal of the American Chemical Society. 1918;40(9):1361-1403.
26. Freundlich H. Über die Adsorption in Lösungen. Z Phys Chem. 1907;57U(1):385-470.
27. Namasivayam C, Kavitha D. Removal of Congo Red from water by adsorption onto activated carbon prepared from coir pith, an agricultural solid waste. Dyes and Pigments. 2002;54(1):47-58.
28. Sharma P, Das MR. Removal of a Cationic Dye from Aqueous Solution Using Graphene Oxide Nanosheets: Investigation of Adsorption Parameters. Journal of Chemical and Engineering Data. 2012;58(1):151-158.
29. Yagub MT, Sen TK, Afroze S, Ang HM. Dye and its removal from aqueous solution by adsorption: A review. Advances in Colloid and Interface Science. 2014;209:172-184.
30. Mahmoodi NM, Hayati B, Arami M, Lan C. Adsorption of textile dyes on Pine Cone from colored wastewater: Kinetic, equilibrium and thermodynamic studies. Desalination. 2011;268(1-3):117-125.
31. Alqadami AA, Naushad M, Alothman ZA, Ghfar AA. Novel Metal–Organic Framework (MOF) Based Composite Material for the Sequestration of U(VI) and Th(IV) Metal Ions from Aqueous Environment. ACS Applied Materials and Interfaces. 2017;9(41):36026-36037.
32. Dragan ES. Design and applications of interpenetrating polymer network hydrogels. A review. Chem Eng J. 2014;243:572-590.
33. Wang S, Sun H, Ang HM, Tadé MO. Adsorptive remediation of environmental pollutants using novel graphene-based nanomaterials. Chem Eng J. 2013;226:336-347.